Hong Kong J Radiol. 2022;25:226-34 | https://doi.org/10.12809/hkjr2217501

PICTORIAL ESSAY

Radiological Features of Rhino-Orbital-Cerebral Mucormycosis Complicating COVID-19 Illness: a Pictorial Essay

NS Chauhan[1], S Kumar[2], P Takkar[1], A Sood[3]

[1]Department of Radiodiagnosis, Dr Rajendra Prasad Government Medical College–Tanda, India
[2]Department of ENT, Dr Rajendra Prasad Government Medical College–Tanda, India
[3]Department of Microbiology, Dr Rajendra Prasad Government Medical College–Tanda, India

INTRODUCTION

Coronavirus disease 2019 (COVID-19) infection has been linked to a myriad of baffling clinical presentations and complications. Mucormycosis has recently emerged as an opportunistic life-threatening invasive fungal infection in patients with COVID-19 infection and is associated with high mortality rates of 50 to 80% in patients who develop intra-orbital or intracerebral disease.[1]

A number of underlying factors are thought to contribute to this high mortality including pre-existing diabetes, over-enthusiastic steroid administration, immunosuppressive therapy, systemic immune alterations due to COVID-19, and the critical health of patients that mandates oxygen support and a prolonged hospital stay.[1-4]

Diabetes mellitus is considered an independent risk factor for mucormycosis infection and also associated with severe disease progression in COVID-19 infections.[5] The underlying reason for this predisposition is the presence of a hyperinflammatory state, delayed interferon gamma response and decreased counts of CD4+ and CD8+ cells. It is speculated that SARS-CoV-2 infection alters innate immunity by affecting CD4+ and CD8+ T cells counts and this state of lymphopenia with immune dysregulation may facilitate development of invasive fungal infection.[6]

Mucormycosis is a broad term used for angioinvasive diseases due to infection with fungi belonging to the Mucorales order. It is chiefly caused by *Rhizopus*, *Mucor*, *Rhizomucor*, *Lichtheimia* and *Cunninghamella* species with *Rhizopus* being the most commonly implicated (Figure 1a and b).[5,6] Spores of mucormycosis are widespread in nature, occurring ubiquitously in the air, soil, organic matter and food. They may exist as commensals in the nasal mucosa of healthy individuals but later germinate in the paranasal sinuses when an individual is immunosuppressed.

The hallmarks of mucormycosis include aggressive and rapid hyphal invasion of tissues, vascular mycotic infiltration, vasculitis, thrombosis and cerebral infarction. Clinically the patient can present with black eschar in

Correspondence: *Prof NS Chauhan. Department of Radiodiagnosis, Dr Rajendra Prasad Government Medical College–Tanda, India*
Email: narvirschauhan@yahoo.com

Submitted: 9 Nov 2021; Accepted: 4 Feb 2022

Contributors: All authors designed the study and acquired the data. NSC and PT analysed the data. All authors drafted the manuscript, and critically revised the manuscript for important intellectual content. All authors had full access to the data, contributed to the study, approved the final version for publication, and take responsibility for its accuracy and integrity.

Conflicts of Interest: All authors have disclosed no conflicts of interest.

Funding/Support: This study received no specific grant from any funding agency in the public, commercial, or not-for-profit sectors.

Data Availability: All data generated or analysed during the present study are available from the corresponding author on reasonable request.

Ethics Approval: All patients were treated in accordance with the tenets of the Declaration of Helsinki. The patients provided written informed consent for all treatments and procedures.

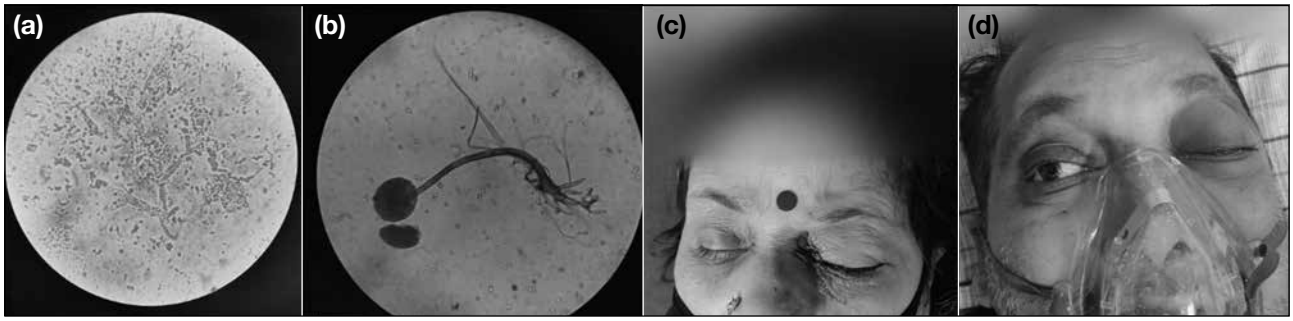

Figure 1. Rhino-orbital-cerebral mucormycosis (ROCM). (a) KOH mount (40×) micrograph showing non-septate fungal hyphae. (b) Micrograph (40×) of a slide culture with lactophenol cotton blue stain showing the typical spherical sporangia, sporangiophore, and rhizoid of Rhizopus. (c, d) Clinical photographs of two patients with ROCM showing (c) blackish discoloration of the left peri-orbital region and nasolabial fold and (d) complete left ptosis with preseptal orbital cellulitis. The patients provided consent for publication of these images.

the nasal cavity/hard palate, nasal blockade, proptosis, chemosis, ptosis, ophthalmoplegia and facial pain (Figure 1c and d).[1] Intracranial extension is heralded by the onset of headache and neurological signs and symptoms.

Radiological investigation is crucial to assess the extent of disease and associated complications. The current radiological description of rhino-orbital-cerebral mucormycosis (ROCM) in concurrent COVID-19 illness is very limited.[3,7,8] The spectrum of imaging characteristics of ROCM in COVID-19 patients is similar to that classically described for ROCM in non-COVID affected immunocompromised individuals. This diagnosis should be strongly considered in patients with COVID-19 infection and suggestive imaging findings, especially when there is corroborative evidence of a concurrent diabetes, steroid administration or need for prolonged intensive care.

In this review, using an anatomical approach, we illustrate the magnetic resonance imaging (MRI) and computed tomography (CT) findings of ROCM from a cluster of microbiologically proven cases diagnosed in our tertiary care hospital in patients admitted with reverse transcription polymerase chain reaction–proven COVID-19 illness.

SINUS DISEASE

Mucormycosis appears as opacification of the paranasal sinuses to a variable extent. The distribution of sinus disease is mostly as pansinusitis (62.5%) or multisinus disease (37.5%) with a left (37.5%) or right-sided predominance (37.5%). The ethmoid sinus is universally affected (100%) and the maxillary sinuses in most (80%) cases.

On CT there is isodense or mixed iso/hypodense attenuation soft tissue opacification or mucosal thickening with either a non-enhancing or mildly enhancing pattern.[9] The MRI imaging findings in sinonasal disease are variable and all sequences such as T2-weighted (T2W), T1-weighted (T1W), T2 fat saturated, and post-contrast T1W fat saturated, should be interpreted in combination. This is particularly important in early-stage disease that is confined to the paranasal sinuses. The signal intensity of the fungal mucosal thickening on T2W images will depend on the proportion of fungal elements that impart a low T2W signal due to paramagnetic effects of iron and manganese and the proportion of necrotic elements that produce a hyperintense signal. On unenhanced T1W, the signal intensity is mostly hypointense or isointense (Figure 2). In a study by Therakathu et al,[9] the percentage distribution of cases displaying varying T2 signals was hypointense/isointense in 37%; heterogenous signal (mixed hypointense and hyperintense areas) in 32% and uniform hyperintense signal in 32%. The signal intensity on T1W was hypointense in all cases. On post-contrast images, the enhancement patterns were non-enhancing/rim enhancing in 36%, heterogeneously enhancing in 36% and homogenously enhancing in 29%.[9]

With its superior soft tissue contrast, MRI may also reveal surrounding bone marrow infiltration in early-stage disease before erosive changes are apparent on CT. Involvement of retro-antral fat should be diligently looked for both on CT and MRI as it is an early sign of soft tissue infiltration.

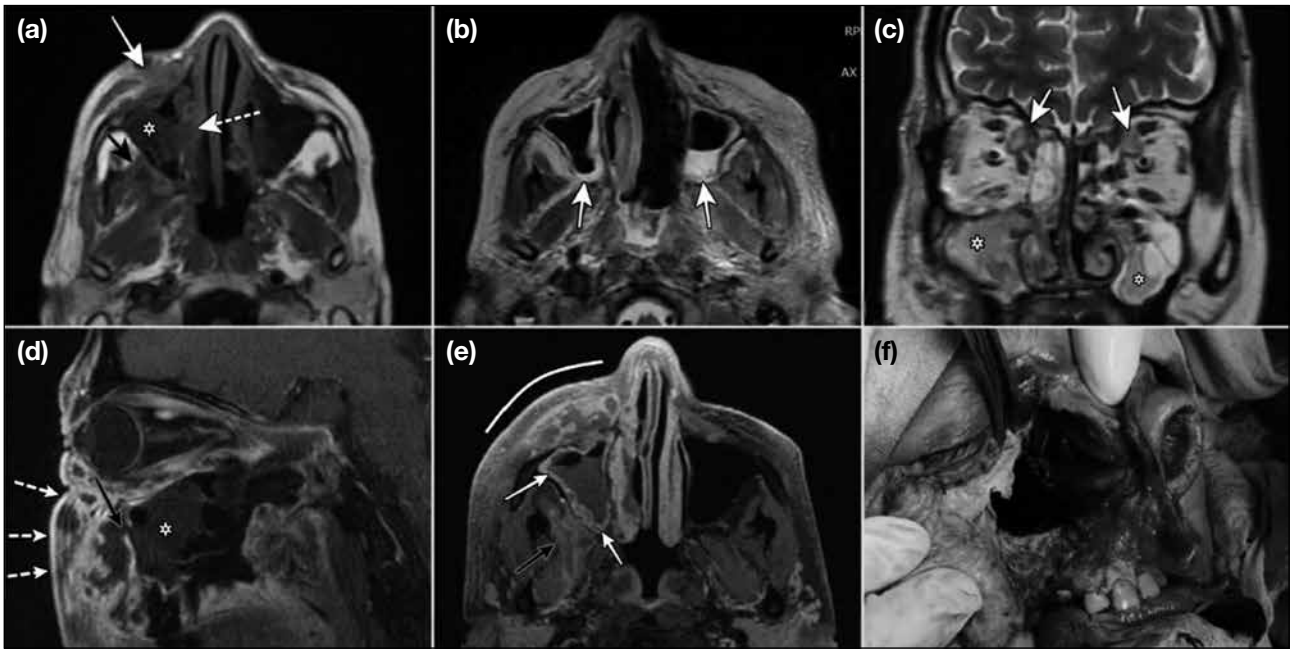

Figure 2. Assorted images from different patients showing sinus disease. Axial (a) T1-weighted and (b) T2-weighted images showing the hypointense signal intensity (asterisk) and hyperintense signal intensity (b; white arrows) of maxillary sinus contents, respectively. Note the premaxillary soft tissue (a; white arrow), encroachment of retroantral fat (black arrow) and subtle involvement of nasal turbinate (white dashed arrow). (c) Coronal T2-weighted image showing the heterogeneous bilateral maxillary sinus contents with admixed low signal (asterisks) and high signal areas. Orbital disease is also present bilaterally (white arrows). (d) Sagittal and (e) axial T1-weighted fat saturated post-contrast images showing non-enhancing pattern (asterisk in d) and peripherally enhancing pattern of the sinus fungal disease. Note the premaxillary soft tissue spread (dashed white arrows, white arc) with bony sinus wall erosion (black arrow in d) and extension to the masticator space musculature (black arrow). (f) Same patient as (e): intraoperative photograph of right maxillectomy showing blackened sinus cavity.

NASAL CAVITY DISEASE

Nasal cavity disease (Figure 3) manifests as soft tissue opacification and/or inflammatory fluid on CT. The middle turbinate is most frequently affected and may show destructive or ulcerative changes. On MRI, a black turbinate sign or a black mucosal sign has been described and refers to non-enhancing mucosa of the nasal turbinate or sinuses respectively on post-contrast MRI. It is considered a feature of early Mucormycosis.[10,11]

EXTRASINUS SPREAD

Non orbital extrasinus spread (Figure 4) can occur in the face, masticator space, premaxillary area, infra-temporal or temporal fossa, retroantral fat, pterygopalatine fossa, or skull base. It is evidenced as fat stranding or soft tissue extension with similar imaging characteristics to intrasinus soft tissue.[9] Although there may be erosive bony destruction in some cases, it is worth noting that in the majority, the extrasinus spread takes place without bony involvement, suggesting a perivascular or perineural route of spread. Extrasinus disease in association with new onset facial/orbital swelling and visual complaints in a COVID-19 patient is a red flag for possible invasive fungal disease.

ORBITAL SPREAD

Orbital spread (Figure 5) commonly occurs through the medial orbital wall and nasolacrimal duct. We found preseptal and/or orbital cellulitis to be a constant feature with involvement of extraconal fat, intraconal fat and the orbital apex as well as the extraocular muscle cone to varying degrees. Oedematous thickening of the extraocular muscle manifests as hyperintense signal intensity of muscle on fluid-sensitive MRI sequences with post-gadolinium enhancement. Medial, inferior, and superior recti muscles are more commonly affected, putatively due to their proximity to the lamina papyracea that is the main route of spread. Sometimes there may be cone-shaped deformation of the ocular globe posteriorly, known as the 'Guitar pick sign', with consequent increased intra-orbital pressure and compromised vision.

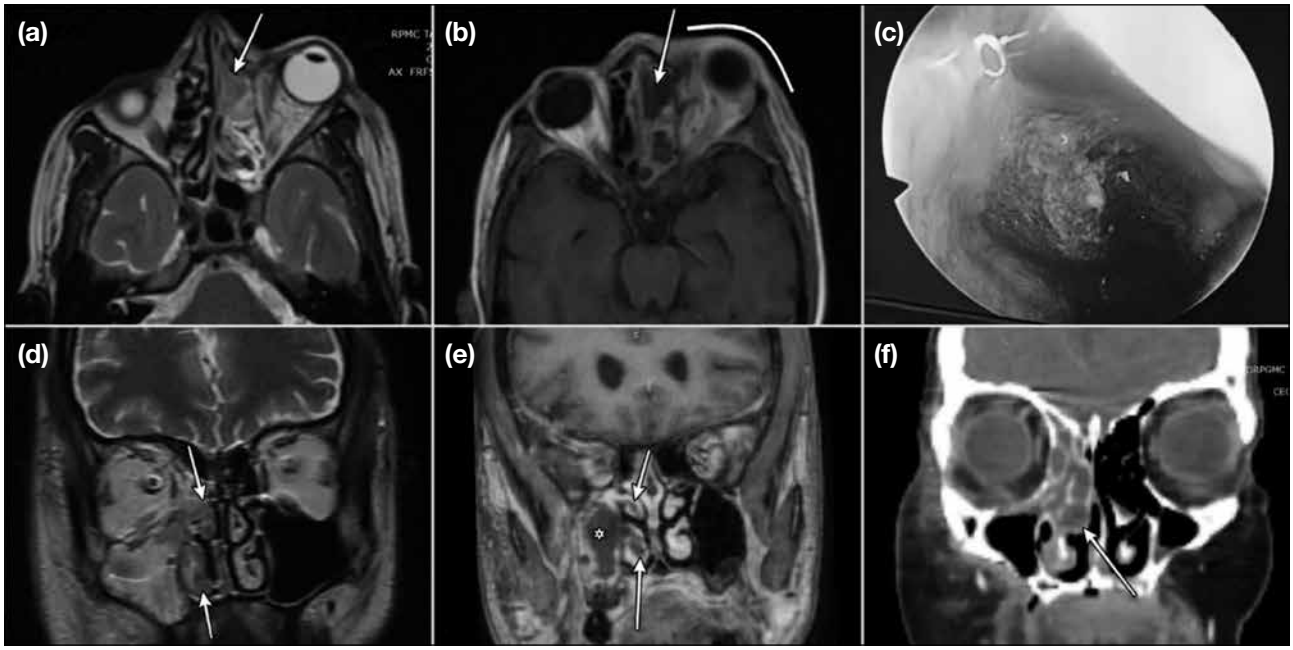

Figure 3. Assorted images from different patients showing sinonasal disease. Axial (a) T2-weighted and (b) T1-weighted post-contrast images showing left ethmoid sinus disease (white arrows) and proptosis of the left globe (white arc). (c) Same patient as (a, b): intraoperative photograph of ethmoidectomy confirming the diagnosis. In a different patient, coronal (d) T2-weighted and (e) multiplanar reconstruction three-dimensional T1-weighted post-contrast images showing fungal involvement of right inferior and middle turbinates with hypointense T2 signal (white arrows in d) and non-enhancement in post-contrast (white arrows in e) s/o black turbinate sign. A contiguous right maxillary sinus disease is also seen (asterisk in e) with non-enhancing contents. (f) Coronal multiplanar reconstruction contrast-enhanced computed tomography image showing the computed tomography equivalent of black turbinate sign (white arrow).

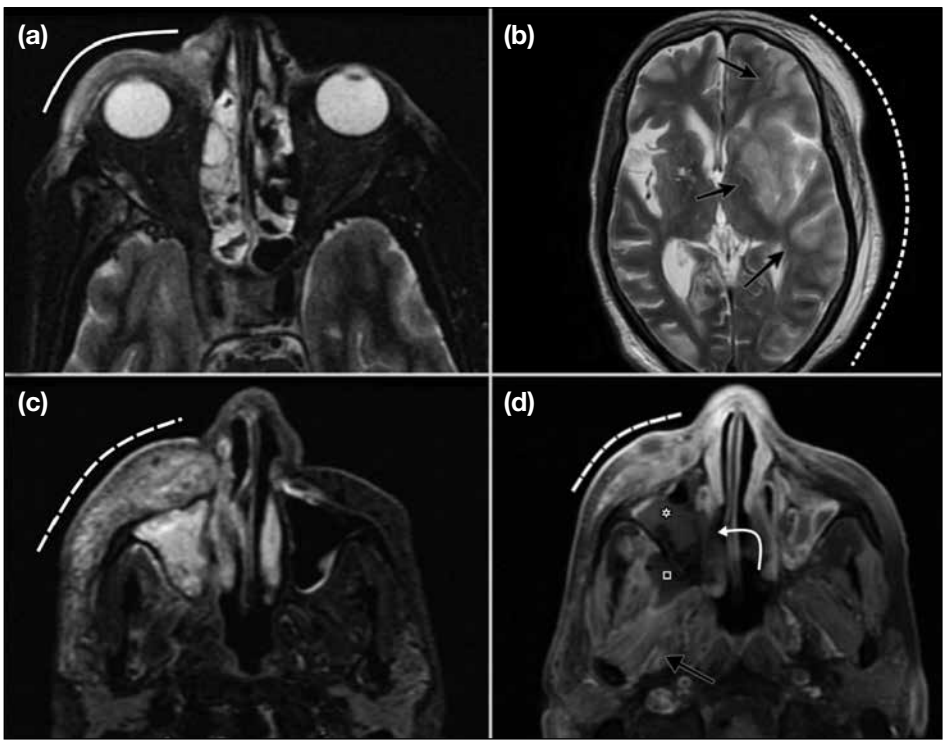

Figure 4. Assorted images from different patients showing perisinus spread. (a) Axial short tau inversion recovery (STIR) image showing preseptal cellulitis (white arc). (b) Axial T2-weighted image showing diffuse scalp oedema (white dashed arc) and left middle cerebral artery territory infarct (black arrows). Axial (c) STIR image and (d) T1 fat-saturated post-contrast images showing premaxillary soft tissue spread (white dashed arc), intrasinus fungal contents (asterisk) with retroantral fat infiltration (white square), masticator space muscle involvement (black arrows) and extension into nasal turbinate (curved arrow).

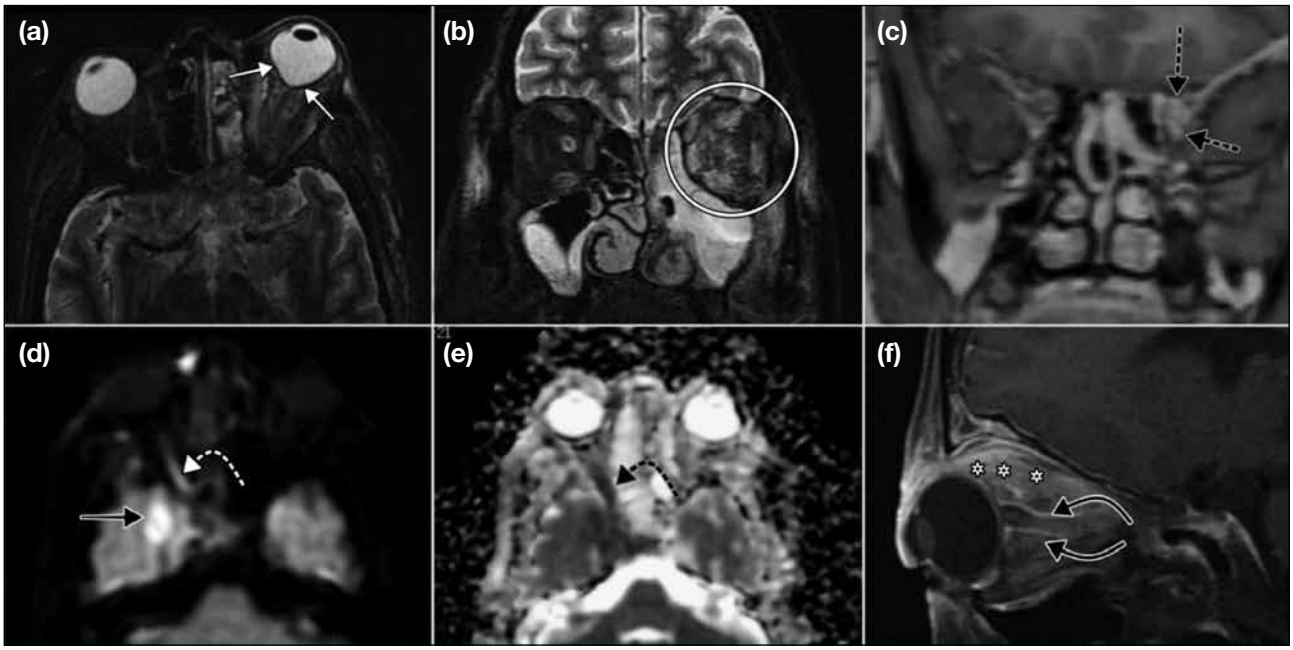

Figure 5. Assorted images from different patients showing orbital spread. (a) Axial short tau inversion recovery (STIR) image showing left proptosis with conical deformation (guitar pick sign) of globe (white arrows). (b) Coronal STIR image showing oedematous thickening and hyperintense signal intensity of extraocular muscles along with intraconal and extraconal fat stranding. (c) Coronal post-contrast T1-weighted image showing the orbital apex involvement (dashed black arrows). (d) Axial diffusion-weighted image and (e) corresponding apparent diffusion coefficient map showing hyperintense signal in the posterior segment of the right optic nerve (curved white dashed arrow) with corresponding dark apparent diffusion coefficient signal (curved black dashed arrow), consistent with optic nerve infarction. A right temporal lobe abscess is also seen abutting the cavernous sinus (d; black arrow). (f) Sagittal post-contrast T1-weighted fat saturated image showing peri-optic enhancement of the optic nerve sheath (curved black arrows) as well as enhancement of the superior rectus muscle (asterisks).

Ischaemic optic nerve infarction has been described rarely in orbital mucormycosis and is probably due to vascular invasion by the Mucor fungus. The posterior intra-orbital segment of the optic nerve is mostly affected and the nerve displays a hyperintense diffusion-weighted imaging signal, and a corresponding hypointensity on apparent diffusion coefficient maps with non-enhancement on post-contrast images.[12]

A circular enhancement around the optic nerve may be observed on contrast-enhanced MRI. This is nonetheless a rarely reported observation in ROCM and may be indicative of perineuritis or direct optic nerve infiltration.[9,13]

CAVERNOUS SINUS INVOLVEMENT

Cavernous sinus (Figure 6) involvement is better assessed on MRI owing to its superior soft tissue contrast. It may manifest as a hypointense intrasinus signal intensity on T1W; mixed hypo/hyper signal on T2W; or non-enhancement/inhomogeneous enhancement in post-gadolinium images with or without features of sinus expansion. It is vital to assess the flow void of the cavernous segment of the internal carotid artery for any signal loss or narrowing of calibre. Internal carotid artery stenosis in the setting of cavernous sinus involvement may be indicative of infectious arteritis and predates a more sinister complication of thrombosis with cerebral infarction in later stages.

PERINEURAL SPREAD

Perineural spread (Figure 7) from the cavernous sinus along the cisternal trigeminal nerve course is exceptionally uncommon in ROCM.[14] On MRI there is thickening with enhancement of the cisternal segment of the nerve that may extend to the pons around the root entry zone. Pontine infiltration may result in infarction, presumably due to associated arteritis or pontine abscess formation with their typical respective MRI imaging manifestations.

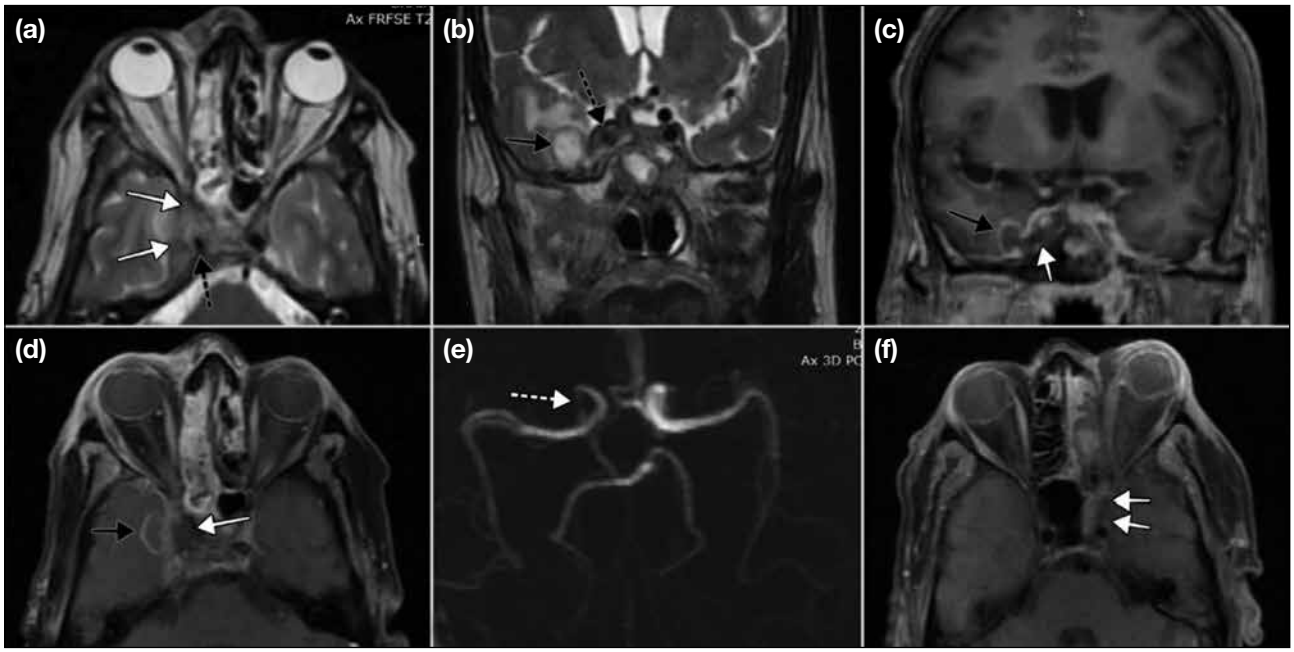

Figure 6. Assorted images from two patients showing cavernous sinus disease. (a) Axial and (b) coronal T2-weighted images showing right cavernous sinus involvement that is expanded (white arrows in a) with heterogenous signal intensity contents. The cavernous internal carotid artery (ICA) displays luminal narrowing and partial loss of signal void (black dashed arrows). (c) Coronal and (d) axial post-contrast T1-weighted images showing lack of enhancement of the right cavernous sinus (white arrow) with adjacent abscess formation in the medial temporal lobe (black arrow). (e) Magnetic resonance angiography image confirms the narrowed calibre of the right cavernous ICA (white dashed arrow). (f) Axial post-contrast T1-weighted image in a different patient revealing an expanded and partially enhancing left cavernous sinus (white arrows).

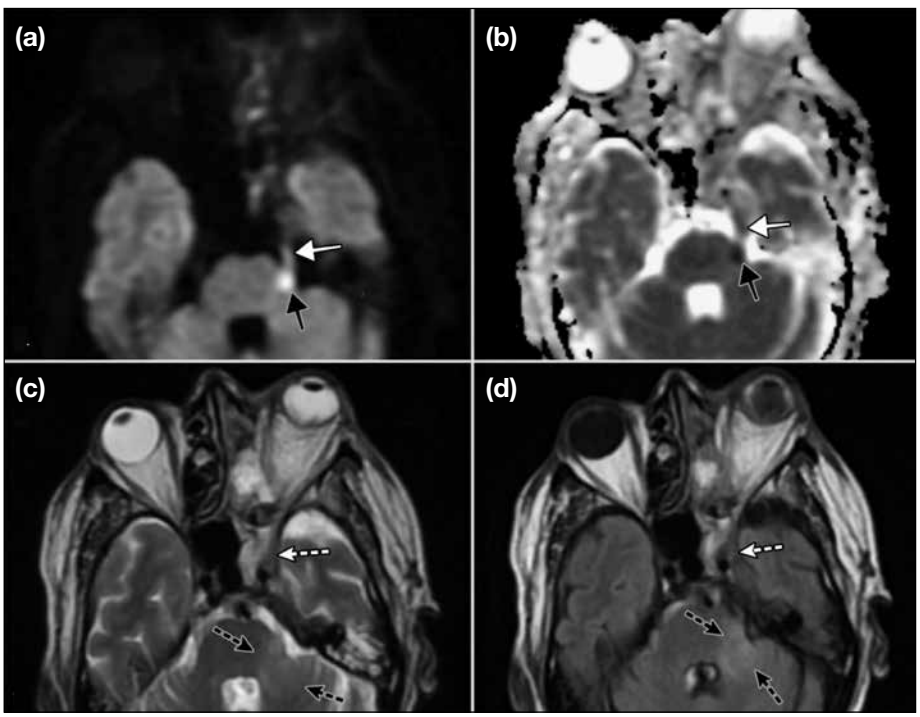

Figure 7. Trigeminal nerve infiltration. (a) Axial diffusion-weighted imaging image and (b) corresponding apparent diffusion coefficient map showing a focal infarct in the left pons at the root entry zone of the trigeminal nerve (black arrow) with similar signal alteration and thickening of the intracisternal trigeminal nerve segment (white arrows) consistent with perineural infiltration. (c) Axial T2-weighted and (d) axial fluid attenuation inversion recovery images showing additional signal abnormality involving the left middle cerebellar peduncle (black dashed arrows) and left cavernous sinus involvement (white dashed arrows).

CENTRAL NERVOUS SYSTEM INVOLVEMENT

Intracerebral extension (Figures 8 and 9) is an ominous development. It may present as cerebritis, cerebral abscess, meningeal enhancement, extradural collections or ischaemia with typical neuroimaging features ascribed to these entities. The imaging appearances of infarcts depend on their acuteness, with the acute/early subacute stage infarctions appearing hypodense on CT and restricting on diffusion-weighted imaging. Parenchymal fungal abscesses resemble the pyogenic ones and show peripheral rim enhancement on contrast enhanced CT/MRI with centrally restricted diffusion. Meningeal enhancement can be dural or leptomeningeal and is better delineated on T1 post-contrast MRI images.

OSSEOUS INVOLVEMENT

Bony involvement (Figure 10) can occur in 40% of ROCM cases and is better demonstrated on CT. The involvement can be as erosions, lytic destruction or thinning with rarefaction and may involve the paranasal bony sinus perimeter or adjacent bony structures such as the pterygoid plates, zygomatic arch and skull base.[9] Erosion of thin lamina papyracea is associated with orbital spread while occasionally erosion of the maxillary alveolus may cause oro-antral fistulisation. Bony erosions, evaluated in combination with other suggestive imaging findings, can be a useful in the diagnosis of invasive fungal sinusitis.[15]

Treatment of ROCM is prompt surgical debridement of the involved area and administration of intravenous antifungal agents. Liposomal amphotericin B is the drug of choice with posaconazole an alternative in cases of resistance/intolerance. The overall prognosis is grim with mortality at 50 to 80%. Presence of brain invasion is associated with even higher mortality rates exceeding 80% but an aggressive surgical approach can be rewarding and has been associated with improved outcome.[1]

CONCLUSION

Opportunistic infections such as ROCM complicating COVID-19 illness in a susceptible patient is a relatively new and dangerous phenomena. It carries a high mortality rate if intracranial complications develop and early identification with expeditious surgical intervention is pivotal in improving the morbidity and mortality.

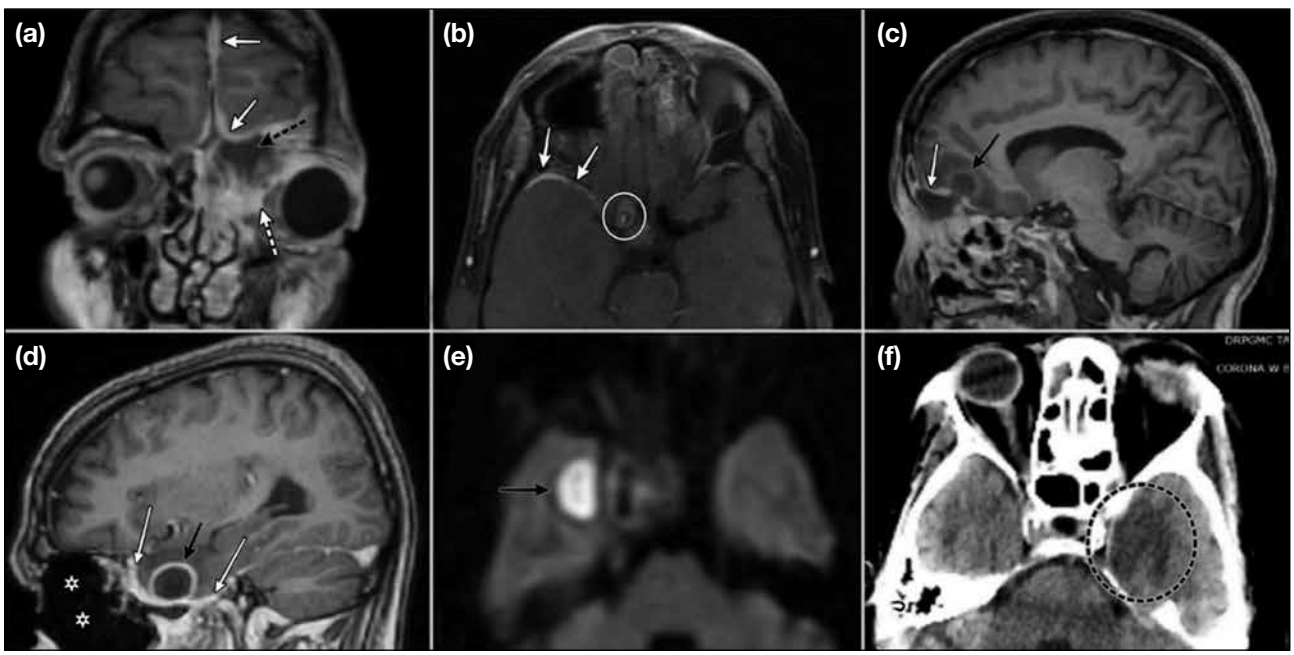

Figure 8. Assorted images from different patients showing intracranial involvement. (a) Coronal and (b) axial post-contrast T1-weighted images showing pachymeningeal enhancement (white arrows) and a thickened enhancing wall of the right supraclinoid internal carotid artery suggestive of possible periarteritis (white circle) along with a partially thrombosed lumen. (a) Note the non-enhancing fungal content in the frontal sinus (black dashed arrow) and orbital extension (white dashed arrow). (c, d) Parasagittal post-contrast T1-weighted images showing brain abscesses with enhancing walls (black arrows) in the (c) frontal and (d) temporal lobes and post exenteration (asterisks). (e) Diffusion-weighted image showing typical restriction (black arrow). (f) Axial non-contrast computed tomography image showing left temporal lobe cerebritis (black dashed circle).

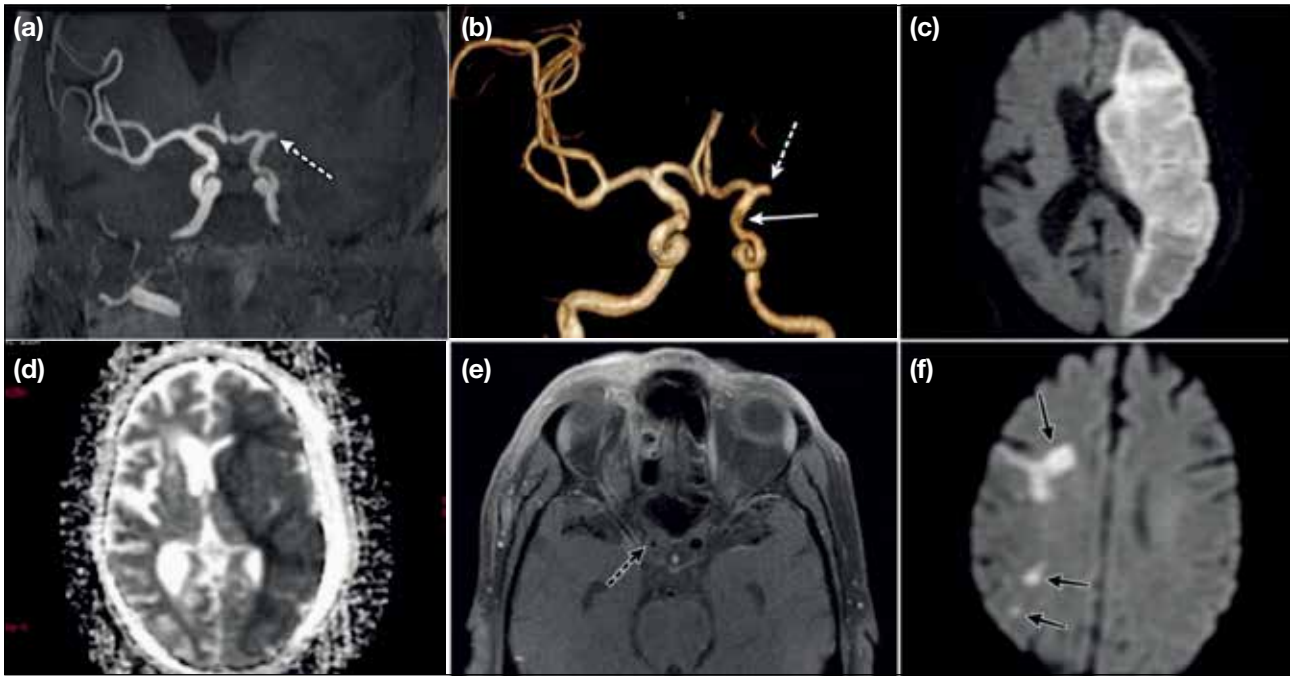

Figure 9. Assorted images from different patients showing intracranial involvement. (a) Coronal maximum intensity projection image and (b) corresponding volume rendered image showing complete occlusion of the left M1 segment (white dashed arrows) with non-visualisation of distal vasculature. The cavernous internal carotid artery (ICA) is narrowed in calibre (white arrow). (c) Diffusion-weighted imaging image and (d) corresponding apparent diffusion coefficient map showing resultant large middle cerebral artery territory infarct. In a different patient, (e) axial post-contrast T1-weighted image and (f) axial diffusion-weighted imaging image showing luminal narrowing of the right supraclinoid ICA (black dashed arrow) with small focal frontoparietal infarcts (black arrows).

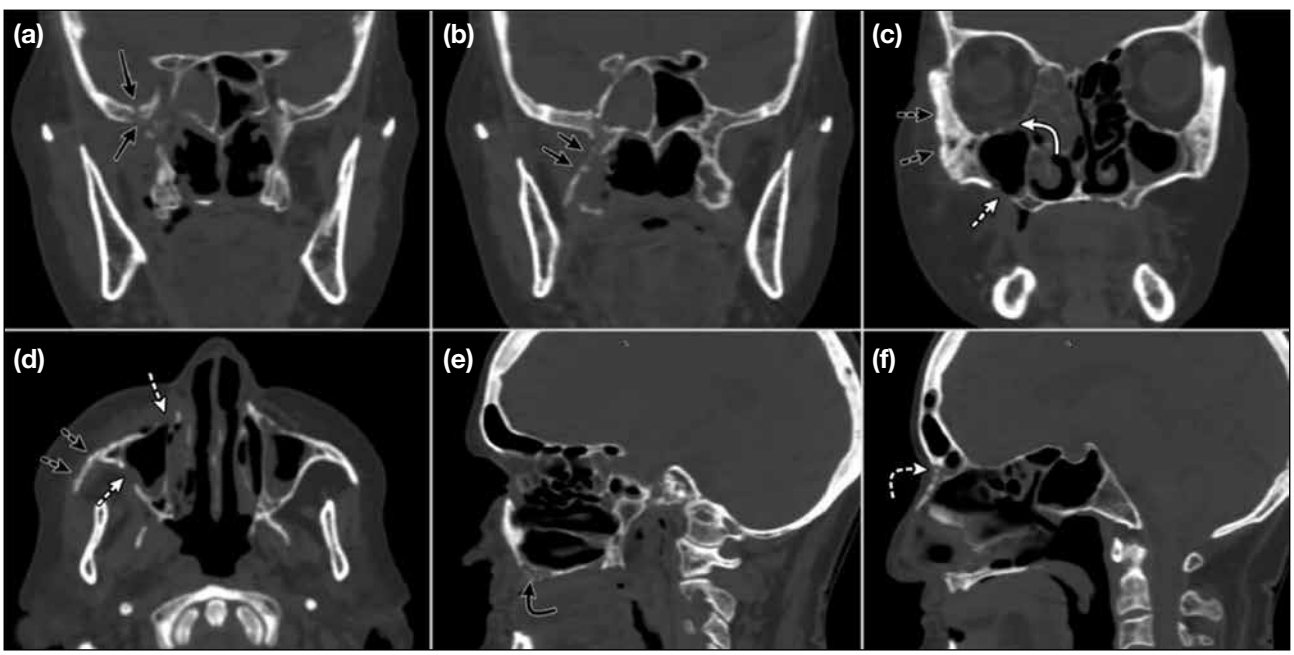

Figure 10. Assorted images from different patients showing osseous involvement. (a-c) Coronal, (d) axial, and (e, f) sagittal multiplanar reconstructed computed tomography images in bone window showing multiple bony erosions involving (a) the right middle cranial fossa (black arrows), (b) lateral pterygoid plate (black arrows), (c, d) maxillary sinus walls (white dashed arrows), (c) lamina papyracea (white curved arrow), (c, d) zygomatic bone (black dashed arrows), (e) hard palate (black curved arrow) and (f) frontonasal bones (white curved dashed arrow).

Radiologists are an important cog in the wheel of multidisciplinary management by virtue of their ability to provide a speedy, accurate diagnosis and elucidate the surgical roadmap.

Radiological diagnosis can be made with a high degree of confidence if attention is paid to the presence of suggestive imaging findings, especially in the subset of patients with COVID-19 who are diabetic or have a history of steroid use or prolonged oxygen or ventilatory support. Radiologists must also be aware of rare manifestations of ROCM such as optic nerve infarction and perineural trigeminal nerve spread.

REFERENCES

1. Sharma S, Grover M, Bhargava S, Samdani S, Kataria T. Post coronavirus disease mucormycosis: a deadly addition to the pandemic spectrum. J Laryngol Otol. 2021;135:442-7.
2. Chen N, Zhou M, Dong X, Qu J, Gong F, Han Y et al. Epidemiological and clinical characteristics of 99 cases of 2019 novel coronavirus pneumonia in Wuhan, China: a descriptive study. Lancet. 2020;395:507-13.
3. Mehta S, Pandey A. Rhino-orbital mucormycosis associated with COVID-19. Cureus. 2020;12:e10726.
4. Garg D, Muthu V, Sehgal IS, Ramachandran R, Kaur H, Bhalla A, et al. Coronavirus disease (Covid-19) associated mucormycosis (CAM): case report and systematic review of literature. Mycopathologia. 2021;186:289-98.
5. Jeong W, Keighley C, Wolfe R, Lee WL, Slavin MA, Kong DC, et al. The epidemiology and clinical manifestations of mucormycosis: a systematic review and meta-analysis of case reports. Clin Microbiol Infect. 2019;25:26-34.
6. Montaño DE, Voigt K. Host immune defense upon fungal infections with mucorales: pathogen-immune cell interactions as drivers of inflammatory responses. J Fungi (Basel). 2020;6:173.
7. Alekseyev K, Didenko L, Chaudhry B. Rhinocerebral mucormycosis and COVID-19 pneumonia. J Med Cases. 2021;12:85-9.
8. Saldanha M, Reddy R, Vincent MJ. Title of the article: paranasal mucormycosis in COVID-19 patient. Indian J Otolaryngol Head Neck Surg. 2021 Apr 22. Epub ahead of print.
9. Therakathu J, Prabhu S, Irodi A, Sudhakar SV, Yadav VK, Rupa V. Imaging features of rhinocerebral mucormycosis: a study of 43 patients. Egypt J Radiol Nucl Med. 2018;49:447-52.
10. Raab P, Sedlacek L, Buchholz S, Stolle S, Lanfermann H. Imaging patterns of rhino-orbital-cerebral mucormycosis in immunocompromised patients: when to suspect complicated mucormycosis. Clin Neuroradiol. 2017;27:469-75.
11. Safder S, Carpenter JS, Roberts TD, Bailey N. The "Black Turbinate" sign: An early MR imaging finding of nasal mucormycosis. AJNR Am J Neuroradiol. 2010;31:771-4.
12. Mathur S, Karimi A, Mafee MF. Acute optic nerve infarction demonstrated by diffusion-weighted imaging in a case of rhinocerebral mucormycosis. AJNR Am J Neuroradiol. 2007;28:489-90.
13. Chen IW, Lin CW. Rhino-orbital-cerebral mucormycosis. CMAJ. 2019;191:E450.
14. McLean FM, Ginsberg LE, Stanton CA. Perineural spread of rhinocerebral mucormycosis. AJNR Am J Neuroradiol. 1996;17:114-6.
15. Middlebrooks EH, Frost CJ, De Jesus RO, Massini TC, Schmalfuss IM, Mancuso AA. Acute invasive fungal rhinosinusitis: a comprehensive update of CT findings and design of an effective diagnostic imaging model. AJNR Am J Neuroradiol. 2015;36:1529-35.